Strongly emissive and photostable four-coordinate organoboron N,C-chelates and their use in fluorescence microscopy

Vânia F. Pais,[a] María M. Alcaide,[a] Rocío López-Rodríguez,[b,c] Daniel Collado,[d] Francisco Nájera,[d] Ezequiel Pérez-Inestrosa,[d] Eleuterio Álvarez,[b] José M. Lassaletta,[b] Rosario Fernández,[c] Abel Ros,*[b] and Uwe Pischel*[a]

Abstract: Six strongly fluorescent four-coordinate organoboron N,C-chelates, containing an arylisoquinoline skeleton, were prepared. Remarkably, the fluorescence quantum yields reach values of up to 0.74 in oxygen-free toluene. The strong B–N interaction was corroborated by the single-crystal X-ray analysis of two dyes. The intramolecular charge-transfer (ICT) character of the fluorophores was evidenced by solvatochromic studies and time-dependent density-functional-theory calculations at the PCM(toluene)/CAM-B3LYP/6-311++G(2d,p)//PCM(toluene)/B3LYP/6-311G(2d,p) level of theory. The compounds combine high chemical stability with high photostability (especially when equipped with electron-donating substituents). The strong fluorescence and the large Stokes shifts predestine these compounds for their use in confocal fluorescence microscopy. This was demonstrated for the imaging of the N13 mouse microglial cell line. As a surplus, significant two-photon absorption cross sections (up to 61 GM) allow the use of excitation wavelengths in the near-infrared region (> 800 nm).

Introduction

Four-coordinate organoboron chelate architectures with tunable strong fluorescence define a landmark at the intersection of organic synthetic chemistry, photophysical design, and optoelectronic applications, such as materials for organic light-emitting diodes (OLEDs), fluorescence imaging, photoswitchable materials, and molecular devices.[1-4] The structural scope includes N,O- and N,N-chelates with five- and six-membered rings as most common binding motifs[3, 5] as well as bi-nuclear boron complexes.[6] Prominent examples are boron 8-hydroxyquinolinate complexes,[7, 8] boron dipyrromethene (Bodipy) dyes,[9-11] boranils,[12, 13] and boron iminocoumarins (Boricos).[14] To a lesser extent organoboron complexes with N,C-chelate systems were reported,[15-19] $B(ppy)Mes_2$ compounds (ppy = 2-phenylpyridyl, Mes = mesityl) being an example.[20] Interestingly, some of the latter were shown to feature reversible photochromic behaviour.[21-24] On the one hand, this switching characteristic is interesting by itself for applications that require the light-induced control of optical properties.[22] On the other hand, such photoreactivity constitutes a severe drawback for applications[22] which require strong light sources or prolonged irradiation times and where photodecomposition should be dimished. Additional molecular design can help avoiding such undesired processes.[22]

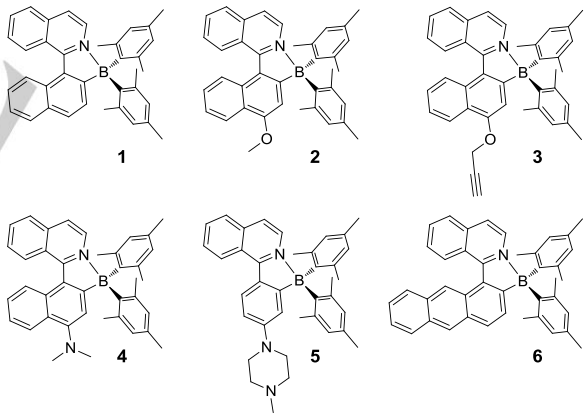

Scheme 1. Structures of the dyes **1**–**6**.

In the present work our interest focused on using arylisoquinolines as alternative N,C chelate ligands. This was motivated by our earlier studies of arylisoquinoline boronic esters (BAI dyes) whose fluorescence properties can be conveniently controlled by the variation of electronic properties of substituents, protonation or temperature.[25-27] The herein investigated N,C chelates (see structures in Scheme 1) feature a higher π-conjugation than the abovementioned photochromic $B(ppy)Mes_2$ compounds.[23] In addition they contain electron-donating substituents and the electron-accepting isoquinolinyl moiety. We anticipated that the resulting excited-state intramolecular charge transfer (ICT) would serve as an energy sink and thereby protect the chromophore from unwanted

[a] Dr. V. F. Pais, M. M. Alcaide, Dr. U. Pischel
CIQSO – Center for Research in Sustainable Chemistry and Department of Chemical Engineering, Physical Chemistry, and Organic Chemistry
University of Huelva
Campus de El Carmen, s/n, E-21071 Huelva (Spain)
E-mail: uwe.pischel@diq.uhu.es
[b] R. López-Rodríguez, Dr. E. Álvarez, Prof. J. M. Lassaletta, Dr. A. Ros
Institute for Chemical Research (CSIC-US)
C/ Américo Vespucio 49, E-41092 Seville (Spain)
E-mail: abel.ros@iiq.csic.es
[c] R. López-Rodríguez, Prof. R. Fernández
Department of Organic Chemistry
University of Seville
C/ Prof. García González 1, E-41012 Seville (Spain)
[d] Dr. D. Collado, Dr. F. Nájera, Prof. E. Pérez-Inestrosa
Department of Organic Chemistry
University of Málaga, IBIMA
Campus Teatinos, s/n, E-29071 Málaga (Spain)
and
Andalusian Center for Nanomedicine and Biotechnology - BIONAND
Parque Tecnológico de Andalucía, E-29590 Málaga (Spain)

Supporting information for this article is given via a link at the end of the document.

photoreactions. Indeed, especially the structures **2**–**5** showed exceptional photostability. Based on the ICT properties, these dyes have large Stokes shifts and good two-photon absorption (TPA) characteristics. These attributes are highly desired for applications in confocal fluorescence microscopy and bioimaging. The four-coordinate situation of the boron center confers increased stability against nucleophilic attack, contrasting the behavior of three-coordinate organoboron compounds.[28-31] The obtained results underpin an improved design of strongly fluorescent and electronically versatile organoboron N,C-chelates and suggest their use in the fluorescence imaging of biological structures.

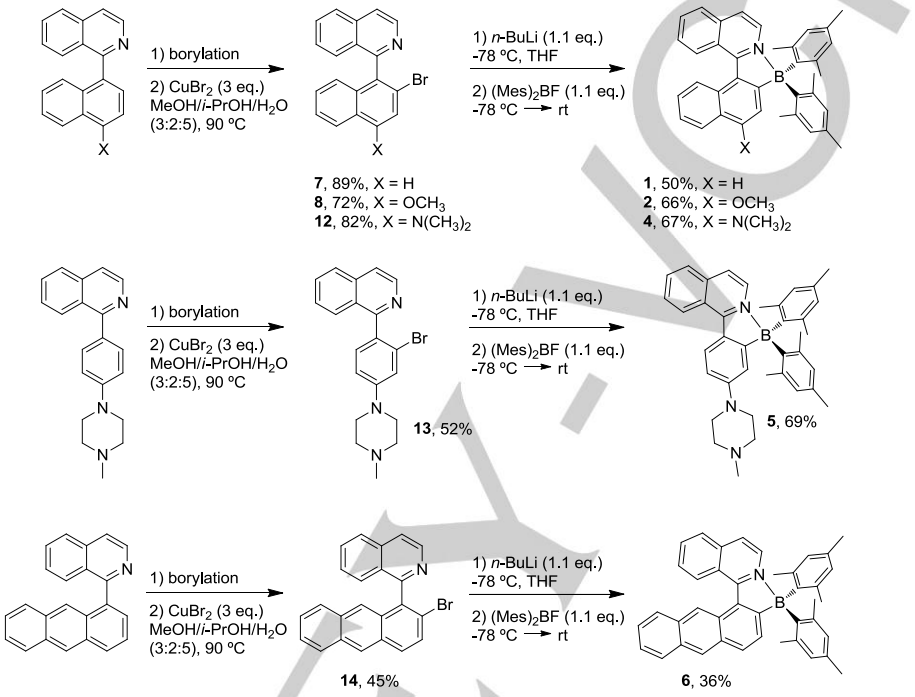

Scheme 2. Syntheses of the dyes **1**, **2**, and **4**–**6**; borylation: B_2pin_2 (1.0 eq.), HBpin (5 mol%), 2-pyridinecarboxaldehyde *N*,*N*-dibenzyl hydrazone (1 mol%), $[Ir(\mu\text{-}OMe)cod]_2$ (0.5 mol%), 55–80 °C.

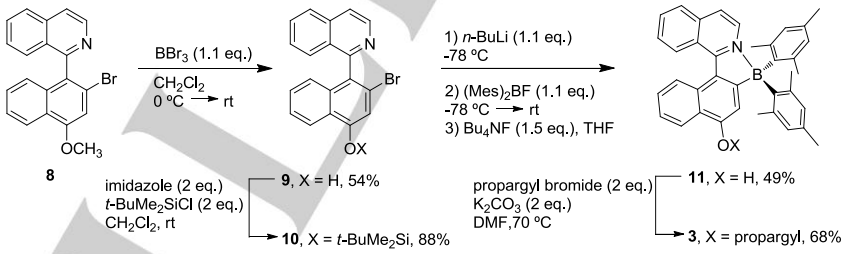

Scheme 3. Synthesis of dye **3**.

Results and Discussion

Syntheses and NMR spectroscopic characterization

The general synthetic approach is based on a recently by some of us described iridium-catalyzed nitrogen-directed *ortho*-borylation of arylisoquinolines that successfully introduces a boryl group in a regioselective manner.[32] The boryl moiety can be subsequently transformed into a bromide using Hartwig´s methodology.[33] This route provides a versatile access to arylbromides that can be converted into the target compounds by a bromide-lithium exchange at −78 °C, followed by trapping of the lithiated species with $(Mes)_2BF$ (Scheme 2).[23] Dye **3** contains a terminal alkyne group that was introduced as potential handle for click reactions[34] in biomolecule conjugation protocols.[35] Starting from bromide **8** this dye was successfully

synthesized by applying a protecting group strategy as outlined in Scheme 3.

The product dyes proved to be air-stable and could be purified by column chromatography on silica gel. They were fully characterized by ^{1}H, ^{13}C, and ^{11}B NMR spectroscopy, high-resolution mass spectrometry, and elemental analysis (see Supporting Information). The ^{11}B NMR chemical shift values of 3.8–5.2 ppm for **1**–**6** are typical for four-coordinate sp^3-hybridized boron atoms resulting from a strong internal B–N interaction.[15, 23] The ^{1}H NMR spectra at 298 K showed broad signals for the mesityl moiety, which is consistent with a slow rotation around the B–C_{Mes} axis. This causes a unequalization of the protons of the mesityl groups. Temperature-dependent ^{1}H NMR measurements with compound **1** as representative example confirm this proposal (see Supporting Information).

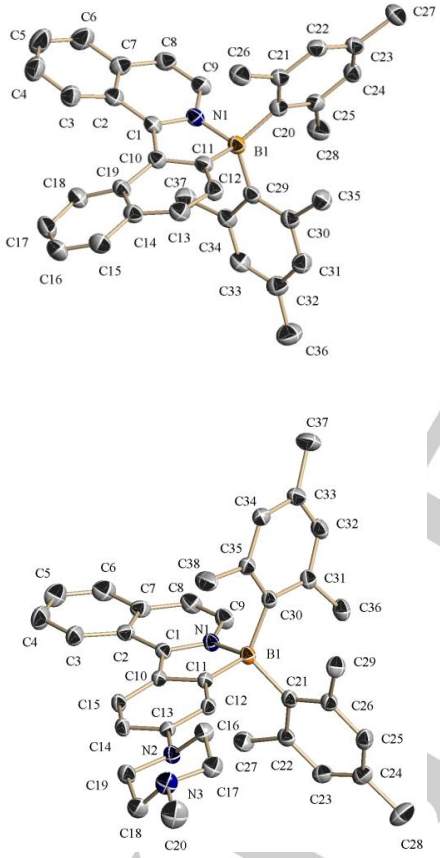

Figure 1. ORTEP diagrams of dye **1** (top) and dye **5** (bottom). The thermal ellipsoids are drawn at the 50% probability level. Hydrogen atoms are omitted for clarity. Selected bond lengths (Å) and bond angles (deg); dye **1**: N(1)–B(1) 1.618(3), C(11)–B(1) 1.627(3), C(20)–B(1) 1.632(3), C(29)–B(1) 1.666(3), N(1)–C(1)–C(10)–C(11) 16.8°, C(2)–C(1)–C(10)–C(19) 27.7°; dye **5**: N(1)–B(1) 1.658(2), C(11)–B(1) 1.619(2), C(30)–B(1) 1.654(2), C(21)–B(1) 1.645(2), N(1)–C(1)–C(10)–C(11) 9.98°, C(2)–C(1)–C(10)–C(15) 14.8°

X-ray crystallography

Fortunately, X-ray quality crystals (see data in Supporting Information) were obtained for **1** by slow evaporation of a solution of the dye in *n*-hexane and for **5** by slow cooling of an *n*-pentane solution. The ORTEP diagrams (Figure 1) show that the boron center adopts a pseudo-tetrahedral geometry with a clear B–N interaction [B–N distance: 1.618 Å for **1** and 1.658 Å for **5**; B–C(11) distance: 1.627 Å for **1** and 1.619 Å for **5**]. This geometry forces the widening of the angles C(2)–C(1)–C(10) (130.7° for **1** and 130.4° for **5**), C(1)–C(10)–C(19) (129.1° for **1**), and C(1)–C(10)–C(15) (129.7° for **5**) with respect to the ideal value of sp^2 hybridized carbons.[36] In contrast to the coplanarity of the two aromatic units in most four-coordinate organoboron N,C-chelates (typical dihedral angles of about 4–7°),[15, 17, 18, 23] the high steric repulsion in **1** forces the isoquinolinyl and naphthyl rings to be twisted around the C(1)–C(10) bond (dihedral angles; N(1)–C(1)–C(10)–C(11) 16.8°, C(2)–C(1)–C(10)–C(19) 27.7°). In consequence a stereogenic axis around this bond is formed.[37] This asymmetry is reflected in the inequivalency of the B(1)–C(20) and B(1)–C(29) distances (1.632 Å and 1.666 Å, respectively) which, together with the hindered rotation of the mesityl rings, may account for the broad signals observed in the ^{1}H and ^{13}C NMR spectra in solution recorded at 298 K. The discussed planarity distortion is less pronounced for dye **5** (dihedral angles; N(1)– C(1)–C(10)–C(11) 9.98°, C(2)–C(1)–C(10)–C(15) 14.8°), providing more symmetry to the structure. This is in accordance with the well-defined signals observed in the ^{1}H and ^{13}C NMR spectra of **5**.

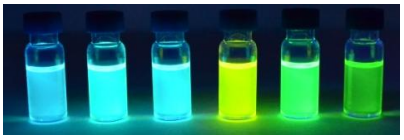

Figure 2. Photograph of the emission colors of the dyes **1**–**6** (from left to right) in toluene under illumination with a handheld UV lamp (365 nm).

UV/vis absorption and fluorescence properties

The photophysical properties of the strongly fluorescent dyes **1**–**6** (Figure 2) in air-equilibrated solutions are summarized in Table 1. Figure 3 shows the optical spectra in toluene; see Supporting Information for other solvents. The UV/vis spectra show rather red-shifted and broad absorption bands with maxima well above 400 nm. The comparison between the dyes **1**, **2**, and **4** clearly demonstrates the influence of the electronic structure of the aryl residue on the absorption-spectral features. The stronger electron-donating the aryl residue, the more red-shifted the absorption band: λ_{max} (**4**) > λ_{max} (**2**) > λ_{max} (**1**). This observation manifests some charge-transfer character of the dyes.

The fluorescence spectra are characterized by broad and structureless bands, whose maxima, depending on the electronic properties of the aryl residue, are encountered between *ca*. 490 and 550 nm in toluene. Again, it was observed that stronger electron-donating residues lead to a

red-shift of the spectral features. Hence, dye **4** shows its fluorescence with a maximum at λ_{fluo} = 547 nm, while dye **1**, the only one being devoid of an additional electron-donor substituent, has the most blue-shifted emission with a maximum at λ_{fluo} = 486 nm.

Table 1. Photophysical properties of **1–6** in air-equilibrated solutions.[a]

		λ_{abs} (nm)[b] [ε ($M^{-1}cm^{-1}$)]	λ_{fluo} (nm)[c]	Φ_{fluo}[d]	τ_{fluo} (ns)[e]
1	TOL	407 [9200]	486	0.35[f]	5.50
	THF	403 [7000]	488	0.30	6.14
	DMF	401 [8600]	495	0.33	7.09
	DMSO	402 [9000]	495	0.33	7.58
	PBS	426 [10800]	503	0.10	3.30[g]
2	TOL	424 [11000]	492	0.62[f]	7.25
	THF	421 [12100]	494	0.62	7.58
	DMF	423 [7700]	500	0.63	7.04
	DMSO	424 [8800]	503	0.67	7.73
	PBS	450 [5700]	498	0.16	2.75[g]
3	TOL	422 [11300]	489	0.61[f]	6.52
	THF	419 [8600]	491	0.64	7.58
	DMF	421 [6400]	495	0.64	7.61
	DMSO	422 [6200]	498	0.65	7.39
	PBS	437 [7000]	501	0.04	0.70[g]
4	TOL	452 [14900]	547	0.52[f]	6.45
	THF	447 [11300]	567	0.49	7.12
	DMF	446 [8200]	585	0.45	7.05
	DMSO	449 [10800]	591	0.48	8.00
	PBS	458 [7200]	570	0.11	2.78[g]
5	TOL	434 [19200]	506	0.43[f]	4.61
	THF	429 [12000]	530	0.31	2.88
	DMF	428 [12800]	545	0.06	0.37
	DMSO	430 [13400]	551	0.05	5.47
	PBS	453 [9000]	533	0.07	6.01[g]
6	TOL	446 [6900]	510	0.15[f]	2.68
	THF	443 [5100]	525	0.10	2.17
	DMF	448 [4900]	540	0.09	2.03
	DMSO	450 [4900]	543	0.09	2.24
	PBS	471 [5000]	544	0.02	0.94[g]

[a] Solvents: toluene (TOL), tetrahydrofuran (THF), *N*,*N*-dimethylformamide (DMF), dimethylsulfoxide (DMSO), 10 mM phosphate buffer saline (PBS, pH 7.4) with 0.1 vol% DMSO as co-solvent. [b] Maximum of the long-wavelength absorption band; the corresponding molar absorption coefficients are given in square brackets. [c] Maximum of the fluorescence emission band. [d] Fluorescence quantum yield; error ±10%. [e] Fluorescence lifetime; error ±5%. [f] Only minor emission quenching by O_2 was noted in toluene (*ca.* 10–15% for **1–3**, **5**, **6** and 30% for **4**). However, by careful bubbling with N_2 the fluorescence quantum yields can be further increased; Φ_{fluo}: 0.40 (**1**), 0.69 (**2**), 0.73 (**3**), 0.74 (**4**), 0.52 (**5**), 0.18 (**6**). [g] Multi-exponential decay, average lifetime according to main components.

While the UV/vis absorption spectra of the dyes vary few with a change of the polarity of the solvent medium (see Table 1 and Supporting Information), very pronounced solvatochromic effects are noted for the fluorescence emission. For example, the fluorescence maximum of dye **4** shifts by about 44 nm upon changing from the non-polar toluene (λ_{fluo} = 547 nm) to the polar dimethylsulfoxide (DMSO; λ_{fluo} = 591 nm) and even by 71 nm when compared with *n*-hexane (Figure 4). Similar observations hold for the dyes **5** and **6** (see Table 1). These solvatochromic effects are compatible with an elevated degree of excited-state intramolecular charge transfer (ICT) that has the locally excited state (LE) as precursor.[38] In agreement with this rationalization, dye **1** shows only minor red-shifted fluorescence emission in polar solvents as compared to toluene ($\Delta\lambda_{fluo}$ = 9 nm in DMSO). In order to underpin the strong charge-transfer character of the fluorescence of dye **4** an extended series of nine solvents was investigated (Figure 4). As shown in Figure 5, the spectral position of the fluorescence maximum can be correlated with the orientation polarizability (Δf) and also with empirical solvent parameters such as the Dimroth-Reichardt parameter [E_T(30)].[39, 40] Furthermore, a Lippert-Mataga plot[41-43] (see Supporting Information) of the Stokes shift *versus* Δf showed a very good correlation and yielded a difference of the dipole moment between the ground state and the excited ICT state of 16 D (Debye) for dye **4**. Further, the ICT character of the investigated dyes was confirmed by time-dependent density-functional-theory calculations at the PCM(toluene)/CAM-B3LYP/6-311++G(2d,p) //PCM(toluene)/B3LYP/6-311G(2d,p) level of theory (see Supporting Information).

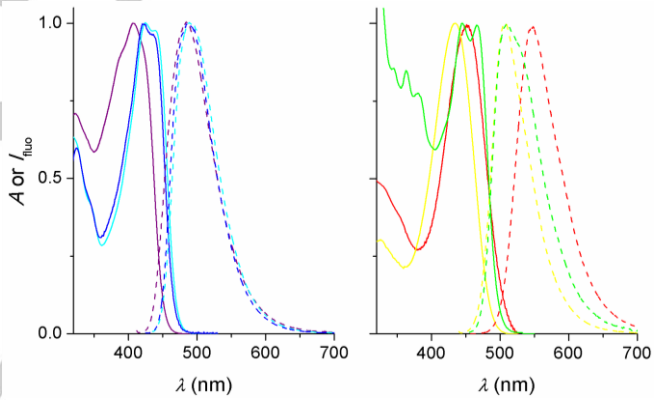

Figure 3. UV/vis absorption (solid lines) and fluorescence spectra (dashed lines) of the dyes **1–6** in toluene; **1**: purple, **2**: cyan, **3**: blue, **4**: red; **5**: yellow; **6**: green.

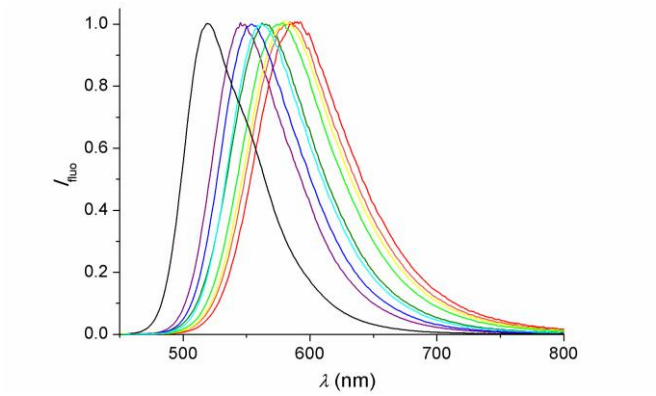

Figure 4. Solvent-dependent fluorescence spectra of dye **4**; *n*-hexane - black, toluene - purple, chloroform - blue, dichloromethane - cyan, tetrahydrofuran - dark green, acetone - green, acetonitrile - yellow, DMF - orange, DMSO - red.

In the cases of the ICT dyes **2**–**4** the fluorescence quantum yields reach values as high as 0.5–0.6 in air-equilibrated toluene solution and also in more polar solvents (see Table 1). In oxygen-free solutions (e.g., in toluene) this can be increased further to values of up to *ca*. 0.7. The dyes **1** and **6** feature generally lower emission quantum yields (see Table 1). The fluorescence lifetimes were found in the range between 4.6 and 7.3 ns, being somewhat lower for dye **6**.

Dye **5** integrates also a lateral electron-donating amino function that is not conjugated to an aromatic moiety. This opens the possibility of photoinduced electron transfer (PET) as additional excited-state process. This has been already verified previously for related borylated arylisoquinoline (BAI) dyes.[26] Expectedly, for such a situation the fluorescence quantum yield should drop in more polar solvents as a consequence of a more favored PET. Indeed, the quantum yield in toluene is 0.43, decreases to 0.31 in the more polar tetrahydrofuran, and finally drops to *ca*. 0.05 in polar solvents such as DMSO, DMF, and acetonitrile. The possibility of PET was further scrutinized by the fluorescence effects upon addition of one equivalent trifluoroacetic acid (TFA); see Figure 6. On the one hand, the protonation of the lateral PET-active piperazinyl N in acetonitrile as solvent yielded a dramatic increase of the fluorescence quantum yield, being 0.43 for the protonated dye (**5**H$^+$). On the other hand, in toluene practically no increase of the fluorescence quantum yield was noted for the protonated dye (Φ_{fluo} = 0.43 for **5** *versus* 0.44 for **5**H$^+$); see Supporting Information.

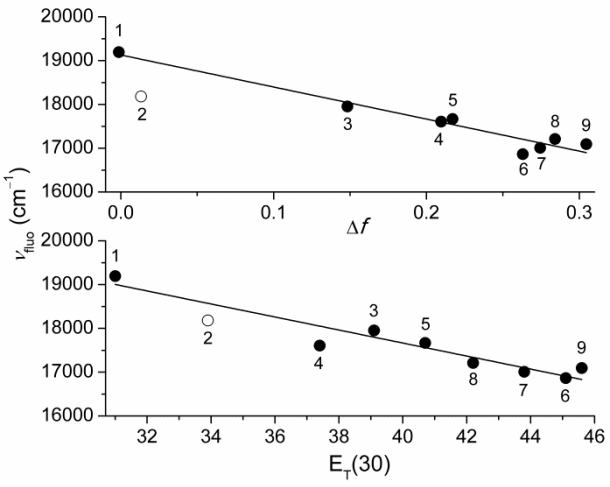

Figure 5. Plot of the emission energy of dye **4** (fluorescence maximum) *versus* the orientation polarizability Δf (top; r^2 = 0.935) and the Dimroth-Reichardt parameter $E_T(30)$ (bottom; r^2 = 0.892); 1 - *n*-hexane, 2 - toluene, 3 - chloroform, 4 - tetrahydrofuran, 5 - dichloromethane, 6 - DMSO, 7 - DMF, 8 - acetone, 9 - acetonitrile. The data in toluene was excluded from the fitting.

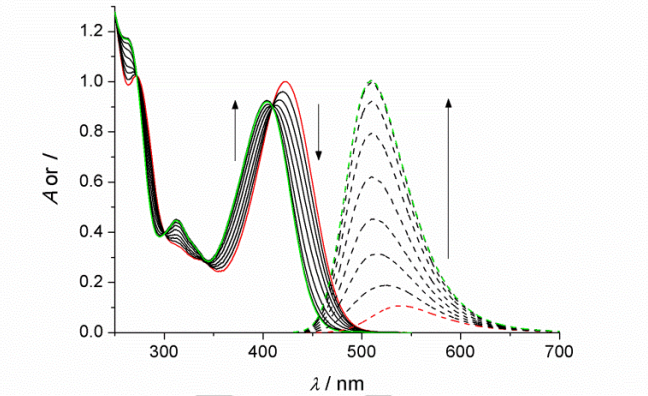

Figure 6. UV/vis absorption (solid line) and fluorescence (dashed line) titration of dye **5** (13 μM) with trifluoroacetic acid (TFA) in acetonitrile; inital spectra in red and final spectra in green. For the fluorescence measurements the sample was excited at the isosbestic point at 409 nm.

The dyes have the observation of a pronounced Stokes shift in common, which varies between 3200 cm^{-1} and 4062 cm^{-1} for **1**–**6** in toluene. In more polar solvents even higher shifts were observed; for example for dye **4** values of 4766 cm^{-1} in tetrahydrofuran or 5408 cm^{-1} in DMSO were obtained. The excited-state ICT process clearly favors the occurrence of large Stokes shifts which is a highly wanted characteristic of strongly fluorescent dyes, such as **2**, **3**, **4**, and **5**H$^+$, in bio-imaging using confocal fluorescence microscopy. In this aspect the herein investigated dyes overcome the often for Bodipy dyes observed small Stokes shifts (*ca*. 500–1000 cm^{-1})[10, 11] which cause problems such as the re-absorption of emitted photons, homo-energy transfer or the undesired detection of strayed excitation light. These shortcomings normally require alternative photophysical designs such as antenna–Bodipy energy transfer dyads.[44-47]

Stability of the fluorophores

For any optoelectronic or biological application the stability of the dyes is of high importance. In order to evaluate this point, a series of experiments was performed that address a) the stability of the B–N bond against nucleophilic attack at the boron center or protonation at the isoquinolinyl N, b) the photochemical stability, c) the stability in buffered solution, and d) the temperature-dependence of the fluorescence emission.

The stability of the B–N bond against fluoride anions as Lewis bases[28, 29] and protons was tested for large excesses (up to 120 eq.) of these reagents. No change in the UV/vis absorption and fluorescence spectra of **1**–**6** in toluene was noted. This underpins the high stability of the four-coordinate chelate.

Recently, the photochromic properties of structurally related B(ppy)Mes$_2$ N,C-chelates were reported by the Wang group.[21-24] In oxygen-free solutions these compounds can be transformed by light irradiation into

borabicyclo[4.1.0]hepta-2,4-diene derivatives. These are then re-converted into the starting material by a thermally activated process. Among the various factors that were shown to influence the photochromic processes of ppy-based organoboron N,C-chelates is the retardation by a) competitive *cis–trans* photoisomerization of attached C=C bond-containing substituents[22] and b) extended π-conjugation of the chelate ligand.[23]

We tested the photochemical reactivity of our compounds in oxygen-free toluene solution under long-term irradiation for 3–4 hours (150 W Xe lamp with a 395 nm or a 420 nm cut-off filter). On the one hand, the dyes **2**–**5** showed no photoreaction under these conditions, being exceptionally photostable. On the other hand, dye **1** and to a much lesser extent **6** yielded irreversible photodecomposition, but no photochromic behavior. Hence, the extension of the aryl π-conjugation alone seems not to improve the photostability. However, the substitution with electron-donating groups provides very photostable dyes (**2**–**5**). It is reasonable to assume that the electron-donor substitution stabilizes the excited ICT state which serves as an energy sink and thereby disfavors competing photoreaction channels.

For bio-relevant applications the compatibility of the dyes with aqueous media is an important asset. The corresponding photophysical data are shown in Table 1. Regarding long-term stability we tested this for the example of **4** (see data in Supporting Information), one of the best-performing dyes in the investigated series. The dye maintains visible fluorescence in 10 mM phosphate saline buffer at pH 7.4 even after 24 hours in solution. Also in confocal microscopy the bright fluorescence of **4** was well observable after this time. The incubation with biomaterials takes usually less than 24 hours, indicating the compatibility of our dyes with most staining protocols. Expectedly, the solubility of the dyes in water is moderate. However, for the purpose of bioimaging a small amount of co-solvent (0.1 vol% DMSO) is already sufficient to enable concentrations of 5–10 μM. At higher dye concentrations aggregation phenomena begin to interfere significantly.

Finally, the dependence of the fluorescence on temperature changes between 283 K and 343 K was investigated in DMF. By comparing the fluorescence quantum yields at the lowest and highest temperature a maximum quenching of *ca*. 15% was observed for the heating of solutions of the dyes **1**, **2**, and **4** (see Supporting Information). The strong B–N interaction limits the rotation around the biaryl axis, thereby making non-radiative deactivation pathways less competitive even at higher temperatures.

Two-photon-absorption (TPA) properties

The two-photon absorption properties of three selected dyes (**1**, **2**, and **4**) with varying ICT character were characterized as well. It is well known that substitution patterns which promote ICT can lead to pronounced non-linear optical phenomena.[48-50] The emission spectra that are observed by two-photon excitation (TPE) resemble the spectra obtained by conventional one-photon excitation (OPE); see Supporting Information. The double-logarithmic plots of the fluorescence intensity *versus* the laser power yield straight lines with slopes between 1.8 and 2.0, thereby confirming the two-photon character of the excitation process (see Supporting Information). By monitoring the emission of the dyes, the TPA spectra and the corresponding cross sections (σ_2) were obtained, using rhodamine B as standard.[48] These spectra are shown in Figure 7. Dye **1** features a broad band with a maximum at *ca*. 800 nm and a σ_2 of 14 GM [1 GM (Goeppert–Mayer unit) = 10^{-50} cm^4 s $molecule^{-1}$ $photon^{-1}$] at this wavelength. The dyes **2** and **4** contain the electron-donating substituent $–OCH_3$ (**2**) or $–N(CH_3)_2$ (**4**) which shifts the TPA maxima to 840 nm and 890 nm, respectively. The σ_2 values at these maxima are 30 GM and 61 GM for **2** and **4**, respectively. As expected, the value increases with an elevated ICT character of the dye. The magnitude of the obtained TPA cross sections, especially the one of dye **4**, compares nicely with that of some of the best performing Bodipy derivatives that were used in TPE fluorescence imaging.[51-53] However, the plain Bodipy chromophore has commonly lower TPA cross sections (*ca*. 10 GM at 900 nm).[47, 54]

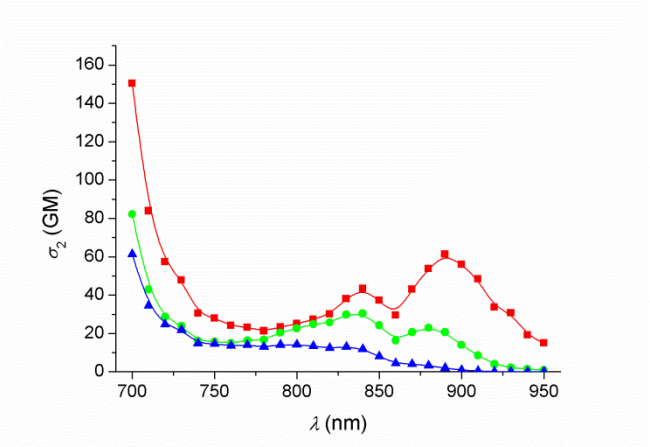

Figure 7. Two-photon absorption spectra of **1** (blue), **2** (green), and **4** (red) in DMF.

Application in confocal fluorescence microscopy

The application of the dyes as fluorescence markers for cellular imaging was tested for the example of dye **4**. The dye was incubated with the N13 mouse microgial cell line for one hour and then submitted to confocal fluorescence microscopy under the conditions of one-photon excitation (OPE) and two-photon excitation (TPE), at λ_{exc} = 458 nm and 900 nm, respectively. Well resolved images (Figure 8) were obtained for both OPE and TPE conditions. The observed emission corresponds to the fluorescence spectrum of the dye, confirming the authenticity of the observed signal. The overlay with the transmission microscopy images clearly shows that the dye is cell permeable

and incorporated in the cytoplasma. The fluorescence intensity is strong enough to allow a reduction of the dye concentration down to 500 nM. The results demonstrate the applicability of **4** as staining dye and the use of TPE is an additional surplus because of the deeper penetration of near-infrared excitation light into biological tissues.[51-55]

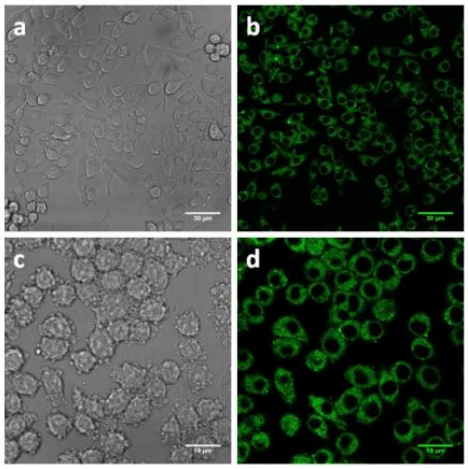

Figure 8. Confocal fluorescence microscopy (pseudo color) of dye **4** (1 μM) incubated with the N13 mouse microgial cell line. Upper row (scale bars: 30 μm): transmission image (a) and fluorescence image under OPE conditions (λ_{exc} = 458 nm, b). Lower row (scale bars: 19 μm): transmission image (c) and fluorescence image under TPE conditions (λ_{exc} = 900 nm, d).

Conclusions

Four-coordinate N,C-chelate organoboranes, that are based on an arylisoquinoline structural motif, were synthesized. Special emphasis was given to the integration of electron-donating substituents in the expectation of promoting intramolecular charge-transfer processes. The occurrence of these processes is confirmed by the observation of broad emission bands, whose maxima depend on the electron-donor strength of the aryl moiety. Additionally pronounced solvatochromic effects are noted. Furthermore, the charge-transfer phenomena are unequivocally confirmed by TD-DFT calculations of the HOMO and LUMO frontier orbitals as well as the ground- and excited state dipole moments.

This study demonstrates that fluorescent labels and probes based on boron chemistry are not limited to the widely explored Bodipy architecture (see Table 2). It has to be admitted that the high molar absorption coefficients are still unmatched by alternative organoboron compounds. However, this is counterbalanced for the investigated dyes by

- increased Stokes shifts,
- high fluorescence quantum yields,
- high chemical and photochemical stability,
- electronic and structural versatility,
- the fine-tuning of the fluorescence by solvent polarity and substitution patterns,
- high two-photon absorption cross sections.

The dyes are charge neutral and have a low molecular mass, which renders them cell permeable. The versatile photophysical and structural properties of the dyes highlight them as an interesting molecular platform to construct functional probes for diverse fluorescence microscopy applications.

Table 2. Comparison of herein investigated organoboron N,C-chelates with the commercial Bodipy FL® dye.

	Organoboron N,C-chelates (1–6)	**Bodipy FL®**[a]
molar absorption coefficient, ε (M^{-1} cm^{-1})	moderate, *ca*. 10000	high, > 80000
excitation/fluorescence (nm)	446/585[b]	503/512
Stokes shift (cm^{-1})	high, up to 5300[b]	low, typically *ca*. 500–1000[c]
fluorescence quantum yield, Φ_{fluo}	high, *ca*. 0.5–0.7	high, *ca*. 0.6–0.9[c]
fluorescence lifetime, τ_{fluo} (ns)	5–7	*ca*. 5–10 ns[c]
polarity-sensitive fluorescence	yes	no
two-photon absorption, σ_2 (GM) at 900 nm	good, *ca*. 60[b]	moderate, *ca*. 10–20[d]
chemical/photochemical stability	high	high
derivatives for bioconjugation	yes	yes

[a] The Bodipy FL® dye is commercialized as a substitute for fluorescein; data from the Molecular Probes® Handbook 2010, except where indicated otherwise. [b] Data for dye **4** in DMF. [c] Ref. 11. [d] Ref. 54.

Experimental Section

Materials: Details on the synthesis, NMR characterization, and crystal structures can be found in the Supporting Information.

Optical spectroscopy: The photophysical measurements were performed on air-equilibrated solutions, typically adjusting an optical density of approximately 0.1 at the excitation wavelength, and using quartz cuvettes with 1 cm optical path length. Where indicated oxygen was removed by bubbling with nitrogen gas. Room-temperature (298 K) UV/vis absorption spectra were recorded with a UV-1603 spectrophotometer (Shimadzu) and the corrected fluorescence spectra were measured on a Cary Eclipse fluorimeter (Varian). The fluorescence quantum yields were determined with 4-amino-*N*-propyl-1,8-naphthalimide (Φ_{fluo} = 0.48 in aerated acetonitrile, this work) as reference, which is used frequently as internal reference in our laboratory. This reference was calibrated before with quinine sulfate in 0.05 M sulfuric acid (Φ_{fluo} = 0.55) as standard.[56, 57] Lifetime measurements were performed by means of time-correlated single-photon-counting (Edinburgh instruments FLS 920) with a picosecond pulsed EPLED 360 (367.4 nm, pulse width at fwhm: 745 ps) or a picosecond pulsed diode laser EPL-445 (442.2 nm, pulse width at fwhm: 78 ps) as excitation light source. The de-convolution analysis of the decay curves yielded the corresponding fluorescence lifetimes.

Steady-state irradiations: The photochemical stability of dyes in nitrogen-purged toluene solution was tested using a 150 W Xenon lamp

(Oriel GmbH & Co. KG). The irradiation light was passed through a 395 nm or a 420 nm optical cut-off filter. Typical irradiation times were 3–4 hours.

Multi-photon microscopy: The fluorescence emission of the dyes **1**, **2**, and **4** in a DMF droplet, loaded on a glass-bottomed dish, was analyzed with an inverted Leica SP5 AOBS MP confocal microscope. As excitation light source a tunable (690–1040 nm) MaiTai Ti:Sapphire HP laser (Spectra-Physics, Inc.) was used. Imaging was done using a 63 × PLAN APO oil immersion objective (NA 1.4) which was focused on the edge of the droplet. This allowed the simultaneous detection of the fluorescence emission of the sample and the background. The spectral data were registered with the Leica LAS AF software. The two-photon-absorption (TPA) cross sections were calculated for a laser power regime where two-photon absorption was secured. For the data treatment a published procedure was followed and rhodamine B (10 μM in methanol) was used as reference.[48]

Cell culture and incubation with dyes: Glass-bottomed cell culture dishes were seeded with the N13 mouse microgial cell line. The cells were cultivated at 37 ºC with 5% CO_2 in Gibco RPMI 1640 medium supplemented with *L*-glutamine (Life Technologies, Inc.) and fetal bovine serum (Life Technologies, Inc.). The procedure was interrupted when 50–70% confluence were reached, which required typically 1–2 days. The N13 cell-containing dishes were incubated for one hour with 1 ml of fresh, preheated RPMI 1640 culture medium containing different concentrations of dye **4** (including a negative control). After incubation the dishes were washed twice with preheated phosphate buffer saline (PBS, pH 7.4) to remove traces of unbound fluorophore and then the cells were fixed using 4% paraformaldehyde for 10 minutes at room temperature. After washing three times with PBS the material was stored at 4 ºC until analysis.

Acknowledgements

The financial support by the Spanish MINECO (CTQ2014-54729-C2-1-P for U.P., CTQ2013-48164-C2-1-P, CTQ2013-48164-C2-2-P for A.R., CTQ2013-41339-P for E.P.I., FPU fellowship for R.L-R., *Ramón y Cajal* contract RYC-2013-12585 for A.R.), the European Union (FEDER), and the *Junta de Andalucía* (2012/FQM-2140 for U.P., 2009/FQM-4537, 2012/FQM-1078 for A.R., postdoctoral contract for V.F.P.) is acknowledged. We are grateful for the access to the Supercomputing and Bioinformatics Center (University of Málaga) and the provided technical support. Tristan Neumann (exchange student from the University of Kiel, Germany) performed preliminary experiments.

Keywords: boron • fluorescence • dyes • charge transfer • multiphoton absorption

[1] C. D. Entwistle, T. B. Marder, *Angew. Chem.* **2002**, *114*, 3051; *Angew. Chem. Int. Ed.* **2002**, *41*, 2927.
[2] O. A. Bozdemir, R. Guliyev, O. Buyukcakir, S. Selcuk, S. Kolemen, G. Gulseren, T. Nalbantoglu, H. Boyaci, E. U. Akkaya, *J. Am. Chem. Soc.* **2010**, *132*, 8029.
[3] Y.-L. Rao, S. Wang, *Inorg. Chem.* **2011**, *50*, 12263.
[4] S. Erbas-Cakmak, O. A. Bozdemir, Y. Cakmak, E. U. Akkaya, *Chem. Sci.* **2013**, *4*, 858.
[5] D. Frath, J. Massue, G. Ulrich, R. Ziessel, *Angew. Chem.* **2014**, *126*, 2322; *Angew. Chem. Int. Ed.* **2014**, *53*, 2290.
[6] Y. Zhou, J. W. Kim, R. Nandhakumar, M. J. Kim, E. Cho, Y. S. Kim, Y. H. Jang, C. Lee, S. Han, K. M. Kim, J.-J. Kim, J. Yoon, *Chem. Commun.* **2010**, *46*, 6512.
[7] Q. Wu, M. Esteghamatian, N.-X. Hu, Z. Popovic, G. Enright, Y. Tao, M. D'Iorio, S. Wang, *Chem. Mater.* **2000**, *12*, 79.
[8] Y. Qin, I. Kiburu, S. Shah, F. Jäkle, *Org. Lett.* **2006**, *8*, 5227.
[9] A. Loudet, K. Burgess, *Chem. Rev.* **2007**, *107*, 4891.
[10] R. Ziessel, G. Ulrich, A. Harriman, *New J. Chem.* **2007**, *31*, 496.
[11] G. Ulrich, R. Ziessel, A. Harriman, *Angew. Chem.* **2008**, *120*, 1202; *Angew. Chem. Int. Ed.* **2008**, *47*, 1184.
[12] D. Frath, S. Azizi, G. Ulrich, P. Retailleau, R. Ziessel, *Org. Lett.* **2011**, *13*, 3414.
[13] J. Dobkowski, P. Wnuk, J. Buczyńska, M. Pszona, G. Orzanowska, D. Frath, G. Ulrich, J. Massue, S. Mosquera-Vázquez, E. Vauthey, C. Radzewicz, R. Ziessel, J. Waluk, *Chem. Eur. J.* **2015**, *21*, 1312.
[14] D. Frath, A. Poirel, G. Ulrich, A. De Nicola, R. Ziessel, *Chem. Commun.* **2013**, *49*, 4908.
[15] A. Wakamiya, T. Taniguchi, S. Yamaguchi, *Angew. Chem.* **2006**, *118*, 3242; *Angew. Chem. Int. Ed.* **2006**, *45*, 3170.
[16] J. Yoshino, N. Kano, T. Kawashima, *Chem. Commun.* **2007**, 559.
[17] J. Yoshino, A. Furuta, T. Kambe, H. Itoi, N. Kano, T. Kawashima, Y. Ito, M. Asashima, *Chem. Eur. J.* **2010**, *16*, 5026.
[18] D. Suresh, C. S. B. Gomes, P. T. Gomes, R. E. Di Paolo, A. L. Maçanita, M. J. Calhorda, A. Charas, J. Morgado, M. T. Duarte, *Dalton Trans.* **2012**, *41*, 8502.
[19] Z. Zhao, Z. Chang, B. He, B. Chen, C. Deng, P. Lu, H. Qiu, B. Z. Tang, *Chem. Eur. J.* **2013**, *19*, 11512.
[20] Y.-L. Rao, H. Amarne, S. Wang, *Coord. Chem. Rev.* **2012**, *256*, 759.
[21] Y.-L. Rao, H. Amarne, S.-B. Zhao, T. M. McCormick, S. Martić, Y. Sun, R.-Y. Wang, S. Wang, *J. Am. Chem. Soc.* **2008**, *130*, 12898.
[22] C. Baik, Z. M. Hudson, H. Amarne, S. Wang, *J. Am. Chem. Soc.* **2009**, *131*, 14549.
[23] H. Amarne, C. Baik, S. K. Murphy, S. Wang, *Chem. Eur. J.* **2010**, *16*, 4750.
[24] N. Wang, S.-B. Ko, J.-S. Lu, L. D. Chen, S. Wang, *Chem. Eur. J.* **2013**, *19*, 5314.
[25] V. F. Pais, H. S. El-Sheshtawy, R. Fernández, J. M. Lassaletta, A. Ros, U. Pischel, *Chem. Eur. J.* **2013**, *19*, 6650.
[26] V. F. Pais, M. Lineros, R. López-Rodríguez, H. S. El-Sheshtawy, R. Fernández, J. M. Lassaletta, A. Ros, U. Pischel, *J. Org. Chem.* **2013**, *78*, 7949.
[27] V. F. Pais, J. M. Lassaletta, R. Fernández, H. S. El-Sheshtawy, A. Ros, U. Pischel, *Chem. Eur. J.* **2014**, *20*, 7638.
[28] Z. M. Hudson, S. Wang, *Acc. Chem. Res.* **2009**, *42*, 1584.
[29] C. R. Wade, A. E. J. Broomsgrove, S. Aldridge, F. P. Gabbaï, *Chem. Rev.* **2010**, *110*, 3958.
[30] Z. Guo, I. Shin, J. Yoon, *Chem. Commun.* **2012**, *48*, 5956.
[31] S. D. Bull, M. G. Davidson, J. M. H. van den Elsen, J. S. Fossey, A. T. A. Jenkins, Y.-B. Jiang, Y. Kubo, F. Marken, K. Sakurai, J. Zhao, T. D. James, *Acc. Chem. Res.* **2013**, *46*, 312.
[32] A. Ros, B. Estepa, R. López-Rodríguez, E. Álvarez, R. Fernández, J. M. Lassaletta, *Angew. Chem.* **2011**, *123*, 11928; *Angew. Chem. Int. Ed.* **2011**, *50*, 11724.
[33] J. M. Murphy, X. Liao, J. F. Hartwig, *J. Am. Chem. Soc.* **2007**, *129*, 15434.
[34] H. C. Kolb, M. G. Finn, K. B. Sharpless, *Angew. Chem.* **2001**, *113*, 2056; *Angew. Chem. Int. Ed.* **2001**, *40*, 2004.
[35] J. A. Prescher, C. R. Bertozzi, *Nat. Chem. Biol.* **2005**, *1*, 13.
[36] A similar widening of the angles (127.0º and 123.6º, respectively) was observed with the formation of a cationic five-membered palladacycle. See: A. Ros, B. Estepa, P. Ramírez-López, E. Álvarez, R. Fernández, J. M. Lassaletta, *J. Am. Chem. Soc.* **2013**, *135*, 15730.
[37] Although Figure 1 only displays the R_a-enantiomer of the dye **1** or **5**, the cell unit contains both enantiomers (see CIF files), since both compounds were obtained as racemates.
[38] Z. R. Grabowski, K. Rotkiewicz, W. Rettig, *Chem. Rev.* **2003**, *103*, 3899.
[39] C. Reichardt, *Solvents and Solvent Effects in Organic Chemistry*, 2nd ed., VCH, Weinheim, **1990**.
[40] C. Bohne, H. Ihmels, M. Waidelich, C. Yihwa, *J. Am. Chem. Soc.* **2005**, *127*, 17158.
[41] E. Lippert, *Z. Naturforsch. A* **1955**, *10*, 541.

[42] N. Mataga, Y. Kaifu, M. Koizumi, *Bull. Chem. Soc. Jpn.* **1955**, *28*, 690.
[43] N. Mataga, Y. Kaifu, M. Koizumi, *Bull. Chem. Soc. Jpn.* **1956**, *29*, 465.
[44] C.-W. Wan, A. Burghart, J. Chen, F. Bergström, L. B.-Å. Johansson, M. F. Wolford, T. G. Kim, M. R. Topp, R. M. Hochstrasser, K. Burgess, *Chem. Eur. J.* **2003**, *9*, 4430.
[45] R. Ziessel, C. Goze, G. Ulrich, M. Césario, P. Retailleau, A. Harriman, J. P. Rostron, *Chem. Eur. J.* **2005**, *11*, 7366.
[46] J. Fan, M. Hu, P. Zhan, X. Peng, *Chem. Soc. Rev.* **2013**, *42*, 29.
[47] D. Collado, P. Remón, Y. Vida, F. Nájera, P. Sen, U. Pischel, E. Pérez-Inestrosa, *Chem. Asian J.* **2014**, *9*, 797.
[48] F. Terenziani, C. Katan, E. Badaeva, S. Tretiak, M. Blanchard-Desce, *Adv. Mater.* **2008**, *20*, 4641.
[49] M. Pawlicki, H. A. Collins, R. G. Denning, H. L. Anderson, *Angew. Chem.* **2009**, *121*, 3292; *Angew. Chem. Int. Ed.* **2009**, *48*, 3244.
[50] Z. Zhang, R. M. Edkins, J. Nitsch, K. Fucke, A. Eichhorn, A. Steffen, Y. Wang, T. B. Marder, *Chem. Eur. J.* **2015**, *21*, 177.
[51] Q. Zheng, G. Xu, P. N. Prasad, *Chem. Eur. J.* **2008**, *14*, 5812.
[52] P. Didier, G. Ulrich, Y. Mély, R. Ziessel, *Org. Biomol. Chem.* **2009**, *7*, 3639.
[53] X. Zhang, Y. Xiao, J. Qi, J. Qu, B. Kim, X. Yue, K. D. Belfield, *J. Org. Chem.* **2013**, *78*, 9153.
[54] C. Xu, R. M. Williams, W. Zipfel, W. W. Webb, *Bioimaging* **1996**, *4*, 198.
[55] W. Denk, J. H. Strickler, W. W. Webb, *Science* **1990**, *248*, 73.
[56] W. H. Melhuish, *J. Phys. Chem.* **1960**, *64*, 762.
[57] W. H. Melhuish, *J. Phys. Chem.* **1961**, *65*, 229.

Entry for the Table of Contents

FULL PAPER

Highly fluorescent and very photostable four-coordinate organoboron N,C-chelates provide a versatile molecular platform for the design of functional dyes with applications in fluorescence microscopy.

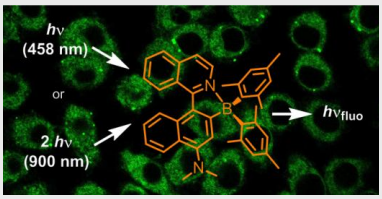

Vânia F. Pais, María M. Alcaide, Rocío López-Rodríguez, Daniel Collado, Francisco Nájera, Ezequiel Pérez-Inestrosa, Eleuterio Álvarez, José M. Lassaletta, Rosario Fernández, Abel Ros, and Uwe Pischel**

Page No. – Page No.

Strongly emissive and photostable four-coordinate organoboron N,C-chelates and their use in fluorescence microscopy